

Characterization of natural resin materials using water adsorption and various advanced techniques

Evangelos P. Favvas · Evangelos P. Kouvelos ·
Sergios K. Papageorgiou · Constantinos G. Tsanaktsidis ·
Athanasios Ch. Mitropoulos

Received: 6 August 2014 / Accepted: 28 January 2015 / Published online: 13 February 2015
© Springer-Verlag Berlin Heidelberg 2015

Abstract A physicochemical characterization of natural raw resin material was evaluated and reported. The studied material is a natural resin, a natural product from *pinus halepensis* trees which is collected from the forests of Chalkidiki region of North Greece. The plurality of this product combined with its special property of removing water from commercial liquid fuels commands the detailed physicochemical characterization of this material. In particular, various techniques, such as water adsorption at 22 °C, thermogravimetric analysis, differential scanning calorimetry, Fourier transform infrared spectroscopy and X-ray diffraction, were used in order to evaluate the structural and surface properties of the material. The water adsorption isotherm was also measured and fitted using the Guggenheim, Anderson and De Boer model in order to correlate the water activity characteristics. In addition, the kinetics of the adsorption was also fitted with good accuracy using the exponential Chapman model. Furthermore, as the results show, the natural resin presents good thermal characteristics. Finally, the studied material presents

efficient water adsorption properties, up to 246.8 mmol/g, and it can be proposed as a promising dehydration material.

1 Introduction

The basic origin of the petrochemistry industry is the mineral sources, petroleum and natural gas. In particular, in our days, fossil feed-stocks in the form of oil (crude oil) and gas (natural gas) are by far the most important raw materials for the chemical industry, representing more than 90 %. In the chemical industry, the larger part of the raw materials is converted to polymers [1, 2]. This is the reason why in the recent years natural renewable products have attracted renewed attention as raw materials for the preparation of resins and other polymeric materials, to replace or augment the traditional petrochemical-based resins and polymers. Natural products such as resins, rubbers and tung oil have found various uses in the painting, varnishes and chemical industries [3].

Until the decade of 70's, Greece was considered as the main resin-producing country of the Europe due to the quantity and the quality of the (oleo)-resin products (turpentine, rosin) collected from the natural forest populations of *pinus halepensis* Mill. Resin, as a secondary forest product, is a natural renewable source which constitutes the basis for the development of hundred of biochemical products, especially now that the chemical industry is rapidly developing. In particular, pine resin, and also oleoresin, represents an inestimable and renewable source of terpenes, showing several industrial applications. For example, turpentine, feedstock, cleaners, pine oil, fragrances and flavoring compounds, pesticides, solvent and thinner for paintings and pharmaceuticals products may be produced by natural resins [4, 5]. Today, it is well

E. P. Favvas (✉) · E. P. Kouvelos · S. K. Papageorgiou
Membranes and Materials for Environmental Separations
Laboratory, Institute of Nanoscience and Nanotechnology,
NCSR “Demokritos”, 153 41 Aghia Paraskevi, Attica, Greece
e-mail: e.favvas@inn.demokritos.gr

E. P. Favvas · A. Ch. Mitropoulos
Hephaestus Laboratory, Department of Petroleum and
Mechanical Engineering, Eastern Macedonia and Thrace
Institute of Technology, 654 04 St. Lucas, Cavala, Greece

C. G. Tsanaktsidis
Laboratory of Qualitative Fuel Control, Department of Pollution
Control and Technologies, Technological Education Institute of
Western Macedonia, 501 00 Kila, Kozani, Greece

established that the natural resin (oleoresin) properties depend on key factors, mostly genetic background and environmental effects [5, 6]. Furthermore, quality (and quantity) of pine resin (oleoresin) and its by-products can be regulated by plant age [5, 7], geographic origin [5, 8, 9] and different stresses, such as drought [5, 10], prescribed fire [5, 11], extreme temperature [5, 12, 13] and flooding [5, 14]. Worldwide, but mostly in China, the pine resins constitute a basic material for the applied medicine market. In particular, the natural resin has been used to treat inflammation, to relieve cough symptoms and to alleviate pain. The pine resin is also used for the treatment of skin diseases, burn and scald wounds, trachitis, pulmonary tuberculosis and as a good antiseptic [15, 16]. Recent studies have indicated that the pine resin mainly consists of the chemical constituents of abietane and pimarane diterpene acids, which were reported to have many biological and pharmacological functions, including antitumor, anti-inflammatory, pesticidal and antibacterial properties, as well as lowering cholesterol and inhibiting ATPase activities [15, 17–22]. On the other hand, the pine natural resins are reported as good candidates for renewable alternative source for bio-fuel [5]. This is supported due to the natural resin high concentration of isoprene, a building block of terpenes, a promising source for bio-fuels and it has already been discussed in community [23]. Therefore, the production of natural resin from pine trees can be an attractive solution in the area of new renewable substitutes of fuel sources. Note that the genetic engineering has been developed in order to increase the production of the isoprene [24].

This work forms the next step of our previous, recent work, where natural resin, from *pinus halepensis* pine trees, was used as a dehydration agent in diesel fuels in order to improve their physicochemical properties [25]. Here, in this work, the used resin is characterized by water vapor adsorption isotherm as well as by various advanced techniques. As we present in the previous work, the natural resin can be used as a good material in order to remove the dissolvent water from the commercial diesel fuels [25]. Here, we investigate the mechanism of this phenomenon, using water adsorption measurement, as well as we study some basic properties of the material, such as the thermal properties, the crystalline properties and some basic

dimensional characteristics of the polymer. The description of the experimental routes and the used instruments as well as the results are all presented and discussed in the following paragraphs.

2 Experimental

2.1 Natural resin material

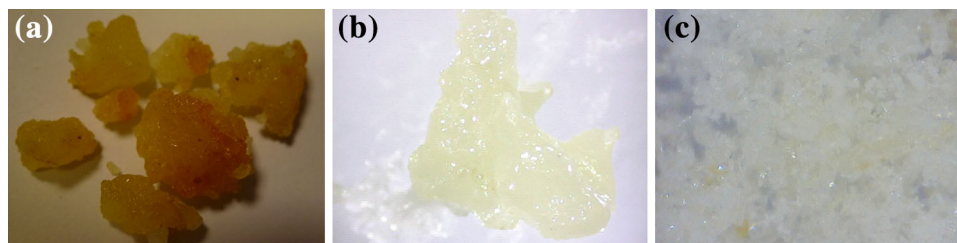
The chosen material for this study is a natural resin from *pinus halepensis* pine trees from the area of Chalkidiki, North Greece (Fig. 1). The resin is a secondary product of pines [26] and generally all conifers, formed in the process of evolution as a defensive mechanism of these species against biotic factors (pathogens, insects, etc.) [27]. The average yield of the selected pine, from which the resin material is derived, is more than 10 kg per year per tree, one of the highest amount worldwide [28, 29].

The resin flows through the resin canals, and it is usually collected by wounding the bark (resin harvesting, tapping). The resin as a natural forestry renewable resource is considered a product of significant economic value worldwide, since it is the raw material for the production of numerous secondary chemical, high-added-value products [30]. The composition of the resin is described previously [25, 31]. In this work, two resin samples were studied and discussed. The first one is the “raw resin” sample which is the material as exactly collected from the pine trees, after the purification of the dirtiness/impurities. The second sample is the “dried resin,” the derivative sample from the “raw sample” which produced after their drying, at inert environment overnight at 100 °C, and was powdered mechanically.

2.2 Characterization techniques

The natural resin, both raw and dried, samples were characterized using various techniques. Firstly, in order to evaluate the water adsorption capacity, adsorption isotherm at 22 °C has taken place and the kinetics were also recorded and discussed. The macroscopic structure of the studied resin materials was evaluated using an optical microscopy. On the other hand, the thermal properties were

Fig. 1 Resin photos. **a** a macroscopic approach of the fresh collected resin from *pinus halepensis* pine trees, **b** picture of the raw sample and **c** picture of the dried powder sample



evaluated using differential scanning calorimetry (DSC) and thermogravimetric analysis (TGA) [25, 32]. The Fourier transform infrared spectroscopy (FTIR) was used in order to evaluate the difference at atomic bonds between the sample before and after the drying. Finally, X-ray diffraction (XRD) technique was performed in order to approach results relevant to the intermolecular characteristics [33, 34].

2.2.1 Water adsorption

The water adsorption isotherm of the dried sample was measured gravimetrically, at 22 °C by means of an Intelligent Gravimetric Analyser (IGA, Hiden Isochema). The sample was outgassed at 80 °C overnight, under ultrahigh vacuum (10^{-7} mbar).

2.2.2 Temperature-modulated differential scanning calorimetry (TM-DSC)

DSC measurements were performed using a temperature-modulated differential scanning calorimetry (TA Instruments, Model MDSC 2920). In order to investigate the temperature where the resin gives the characteristic phase transitions, the DSC technique was used for both raw and dried resin samples. Both runs were undertaken using a heating ramp of 2 °C/min, a cooling rate of 5 °C/min and a temperature modulation of ± 0.32 °C every 60 s.

2.2.3 Thermogravimetric analysis (TGA)

TGA spectra were obtained in a TGA/DTA–DSC Thermogravimetric–Differential Thermal Analyzer (Setaram, Setsys Evolution 18). Both resin samples (~ 70 mg) were heated from room temperature up to 600 °C in platinum crucibles, with the same linear heating rate of 2 °C/min. The furnace was fed with 20 cm³/min pure Ar, while the heat flow rate was kept constant throughout the pyrolysis process. The temperature increased from 25 to 120 °C in steps of 2 °C/min. The samples were left at 120 °C for 30 min in order to remove any absorbed water molecules, volatile impurities and any trace of solvents. Then the following pyrolysis protocol was applied: heating rate of 2 °C/min up to 600 °C, stabilization at the maximum

temperature for 30 min and then controlled quenching at a cooling rate of 10 °C/min down to 25 °C.

2.2.4 Fourier transform infrared (FTIR) spectrum analysis

FTIR spectra of both resin samples, raw and dried, were recorded using a horizontal ATR Trough plate crystal cell (Thermo Electron 6700 ATR diamond) equipped with a Nicolet 6700 FTIR (Thermo Electron Corporation) operating at room temperature. For the spectra analysis, the samples were placed on the crystal cell, which was in turn mounted on the spectrometer. The spectra in the range of 400–4,000 cm⁻¹ were scanned and the automatic signals were collected. The background spectrum was recorded at room temperature with an empty cell.

2.2.5 X-ray diffraction

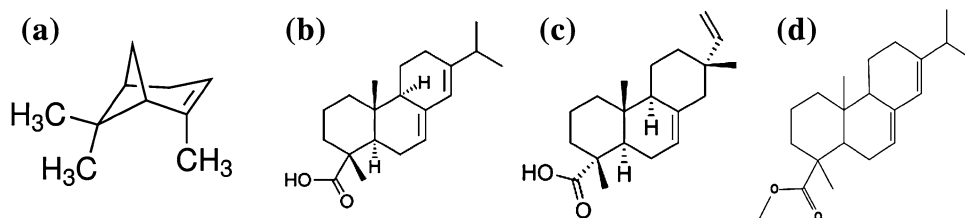
The X-ray diffraction (XRD) patterns were recorded on a Siemens XD-500 diffractometer using CuK α X-ray source. Both samples were put into the standard XRD powder cell and the experimental time for the XRD spectra was about 8 h.

3 Results and discussion

3.1 Natural resin

As a chemical compound, the resin is a mixture of terpenoids and fatty acids [25]. Some of these compounds are volatile (turpentine) and others nonvolatile (resin). Among the terpenoids, the monoterpenoids and the sesquiterpenoids constitute the volatile part that is the 15 % of the total resin weight and they are the components of turpentine. These resins are a natural polymer product, which can be reported as a blend of terpenes (monoterpenes and diterpenes), whose basic building block is the isoprene, a substance with five carbon atoms and eight atoms of hydrogen (C₅H₈), which could “generate” hydrogen bonds with water molecules, also in diterpenes via charged groups (carboxyl groups) and dynamic absorption of water molecules (Fig. 2). Due to these molecules, the water molecules can be adsorbed at high amounts based on physical

Fig. 2 Chemical structure of a-pinene molecule (a), abietic acid molecule (b), isopimaric acid (c) and methyl abietate–abietic acid (d)



adsorption mechanisms mainly on the active “points” on the surface of the material.

The main chemical composition of the studied natural resin is: monoterpenes 32.9 % (α-pinene 30.72 %), sesquiterpenes 1.26 % (unresolved diterpene aldehyde (M = 286) 0.52 %, primaric acid 0.41 % and cyclohexanecarboxylic acid 0.29 %) and diterpenes 65.84 % (methyl abietate + abietic acid 39.93 %, palustric acid 9.57 %, isopimaric acid 5.87 % and abietic acid 5.71 %) [25, 31].

3.2 Water adsorption analysis

The mass changes during the adsorption process can be described as a function of time during the equilibrium at each relative pressure P/P_0 by the follow equation:

$$q(t) = Q \left[1 - \exp\left(\frac{-t}{B}\right) \right] \quad (1)$$

where $q(t)$ is the change of sample mass (g/g) in terms of time, t is time in min, Q represents the water adsorption capacity at equilibrium, and B is time, in min, for the adsorption of half the amount of water adsorption capacity at equilibrium ($B = t$, when $q(t) = Q/2$).

The relationship between water vapor adsorption capacities and equilibrium relative humidities can be described by the Guggenheim–Anderson–de Boer model (GAB) with the three parameters, according to Eq. 2.

$$M = \frac{(M_0 C k a_w)}{(1 - k a_w)(1 - k a_w + C k a_w)} \quad (2)$$

where C is the Guggenheim constant, k is a constant correcting the properties of the multilayer molecules with respect to the bulk liquid, M is the equilibrium water content (% dry basis), and M_0 is the monolayer moisture content (% dry basis) [35]. Based on these approximations, both kinetics and isotherm curves were fitted with the particular models and the specific parameters were calculated using the Origin software.

The water adsorption capacity of the resin material was first characterized by the kinetics of water during equilibrium at different relative pressures (relative humidities) from 0 to 95 % at 22 °C. The kinetic curve is observed in a typical exponential shape and the equilibrium time is vibrated from ~ 81 min, at the first equilibrium point of $P/P_0 = 0.06$, up to ~ 300 min for $P/P_0 = 0.95$. In order to fit better the experimental data, the Chapman exponential model is applied [36], Eq. 3, and both the experimental and calculated data of the first equilibrium point presented in Fig. 3. Here in Eq. 1, one additional parameter, L , has been added as exponent in the second part of the equation. Specifically, the Chapman model is described as follows:

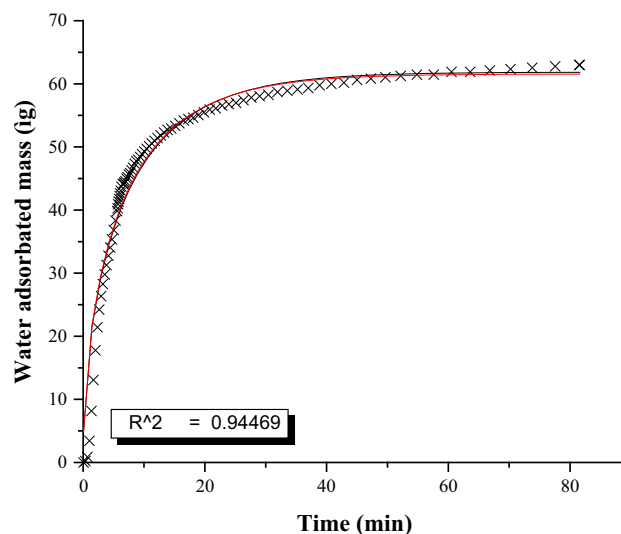


Fig. 3 Kinetics of water vapor adsorption for dried resin sample at 22 °C in case of an increased RP (relative pressure) from 0 to 6 %. Experimental points (×) and calculated curve (–) by the exponential Chapman model

$$q(t) = Q \left[1 - \exp\left(\frac{-t}{B}\right) \right]^L \quad (3)$$

where again $q(t)$ is the change of sample mass (g/g) in terms of time, t is the time in min, Q represents the water adsorption capacity at equilibrium, B is the necessary time, in min, for the adsorption of the half amount of the total water adsorbed amount ($B = t$, when $q(t) = Q/2$), and L is an extra function for the curvature correction of the curve.

For each relative pressure, the change in sample mass follows, as a function of the time, the exponential route according to Eq. 3. The model parameters were calculated as: $Q = 61.57(\pm 0.78356)$, $B = 10.92(\pm 0.00501)$ min and $L = 0.5$, indicating that the total amount of water adsorbed reaches 61.85 μg while half was adsorbed during the first 10.92 min of the process.

As observed in Fig. 3, the calculated values of water adsorption capacity are very close to the experimental values. Good fitting of the experimental data, with similar accuracy, was also observed for all other equilibrium steps, $P/P_0 = 0.06$ to $P/P_0 = 0.95$, (data not shown).

The water adsorption isotherm (both adsorption and desorption branches) is presented in Fig. 4. The equilibrium moisture content increased with increasing water activity following a shape typical of vapor adsorption corresponding to type III isotherms according to the Brunauer’s classification [37] with total amount of water adsorbed reaching 0.0137 g/g or 246.8 mmol/g. This uptake value is close to what was reported by other researchers for natural materials [35], higher than activated carbons [38] but lower than silicate mesoporous structures [39].

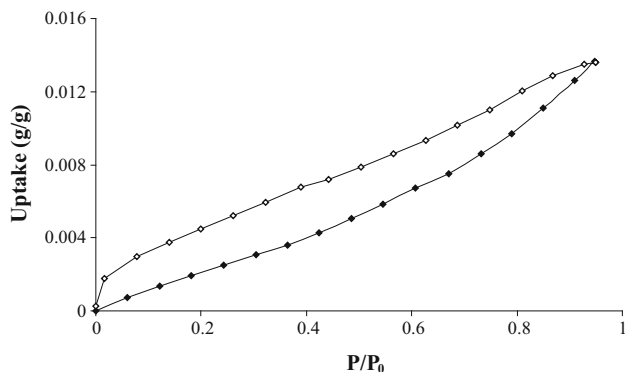


Fig. 4 Water vapor adsorption/desorption isotherm of the dried resin sample at 22 °C

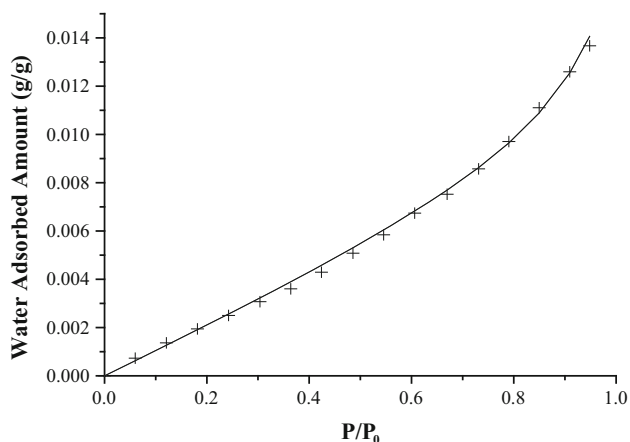


Fig. 5 Comparison between experimental water vapor adsorption isotherm and predicted water vapor adsorption isotherm at 22 °C. Experimental points (+) and calculated curve (–) by the GAB model

The water desorption from dried resin sample showed quite significant hysteresis in agreement with previous studies concerning other natural and synthetic materials, such as montmorillonite [40] and copolymers [41]. However, as shown in Fig. 4, the hysteresis loop is wide at relative pressure of 90 %. The hysteresis is maintained although narrower down to the lower relative humidity $P/P_0 \cong 0$. This remaining amount of water cannot be removed except by outgassing at room temperatures. Similar behavior of the desorption branch has also been observed in sepiolite materials [42]. This phenomenon is observed in systems, where the adsorbate does not condense in mesoporous channels but forms clusters of water molecules nucleated on active centers of the surface.

In Fig. 5, experimental and predicted, by the GAB model, water adsorption isotherms are compared at 22 °C. The adsorption isotherm has a sigmoidal shape indicating a two-step humidity adsorption process [43–46].

During the first step, up to $\sim P/P_0 = 0.45$, a linear region is observed during monolayer and subsequent

multilayer stacking of water molecules, followed by a second region where water clusters begin to form leading to a steeper adsorption curve. The experimental data were fitted, with very good accuracy, $R^2 = 0.998$, using the GAB model, and the model parameters were calculated obtaining the following values: monolayer water content, $M_0 = 0.15946$, Guggenheim constant $C = 0.07171$ representing the heat of sorption for the formation of the first layer and $K = 0.9049$. The values of k ($K < 1$) and the correlation coefficient ($R^2 > 0.98$) showed that the GAB equation is an adequate equation for fitting experimental data for starchy films, as previously reported by other authors [47, 48].

3.3 Temperature-modulated differential scanning calorimetry (TM-DSC)

The characteristic transition temperature, T_g , is about 37 °C (data not shown). In addition, the raw resin sample exhibits an endothermic peak at 127 °C due to desorption of the strongly adsorbed humidity followed by a second, smaller endothermic peak at 144 °C when the volatile components start to “crawl.” In the case of the dried resin sample, the first peak does not occur at 127 °C and the second is shifted to the right due to the heating pretreatment. The main endothermic peak, for both samples, can be observed at temperatures over 240 °C.

These curves can be attributed to the relaxation, deformation and finally the degradation of the polymeric chains. Particularly in the case of the raw resin sample, the required heat (energy) is 198.7 J/g, while it is 85 J/g in the case of the dried sample. This difference in required energy of the chain relaxation occurs due to the reordering of the polymeric chains during heating for the drying of the sample. As shown in Fig. 6, the peaks of these endothermic curves appeared at 247 and 262 °C for the dried and raw resin samples, respectively. These temperatures can be reported as the melting transition points for each studied sample.

3.4 Thermogravimetric analysis (TGA)

For our carbonization experiments, argon was chosen as a pyrolysis gas since it is considered the best non-active gas for polymeric precursor materials; it results to a milder activation action than it is possible with other gases such as helium or nitrogen [49].

As we can see in Fig. 7, there are three main weight-loss stages for both resin samples. The first weight loss region occurs up to 300 °C when the two curves are identified “instantaneously.” The weight loss of the raw resin sample was recorded strongly due to the removal of the adsorbed humidity as well as the evaporation of the volatile and

Fig. 6 DSC curves of the raw natural resin and the dried resin sample

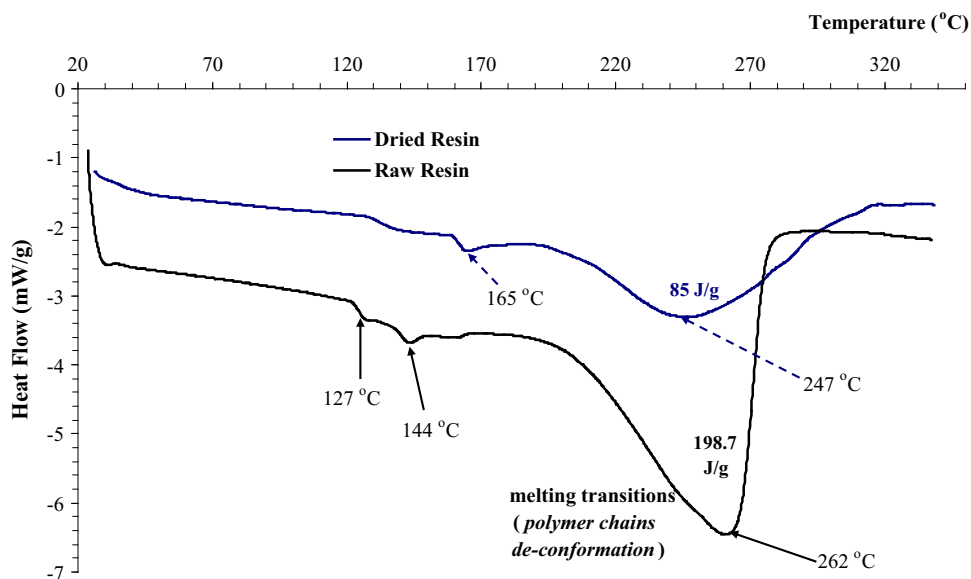
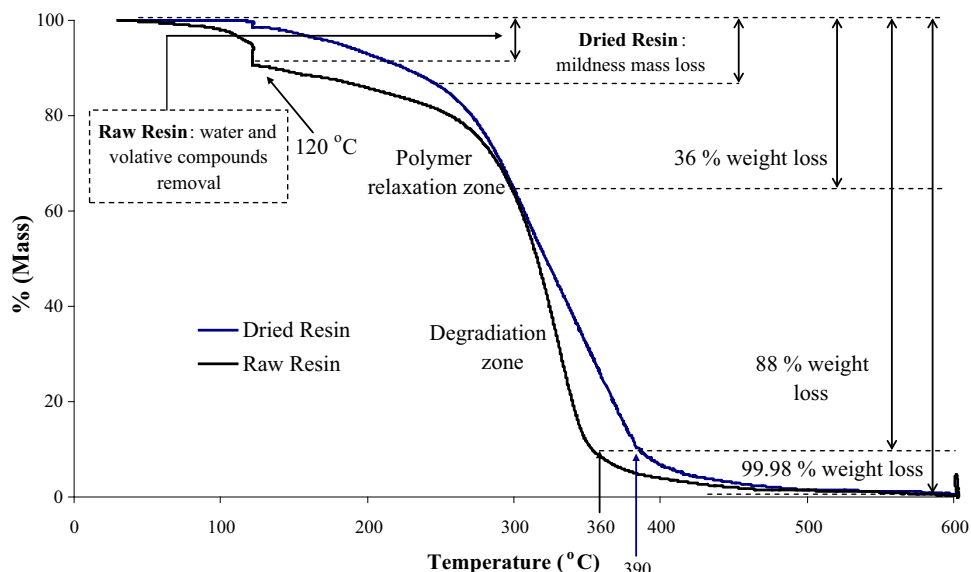


Fig. 7 TGA curves of the raw (black line) and the dried (blue line) resin samples

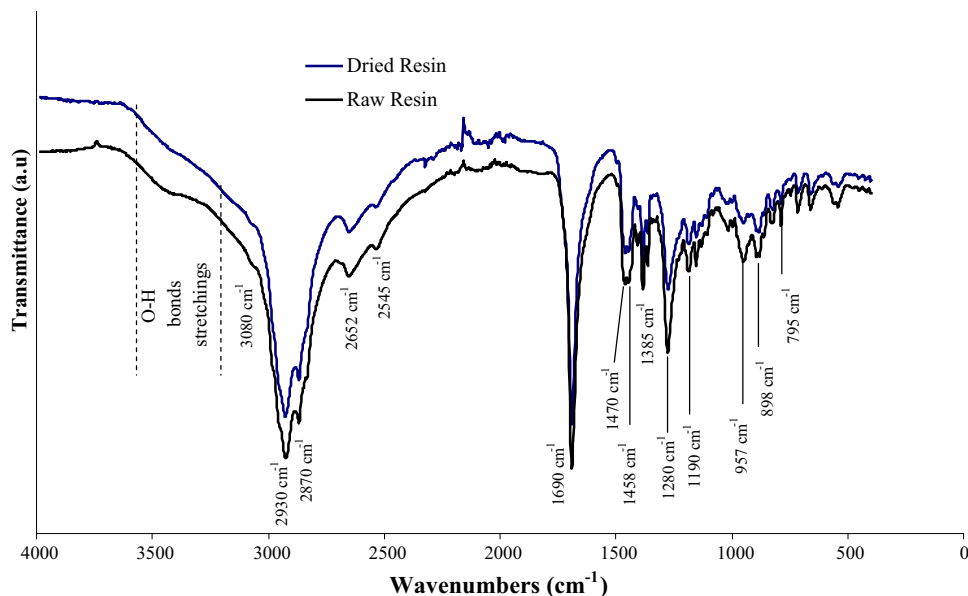


“stronger” components (the boiling point of α -pinene, the main compound of monoterpenes, is $156\text{ }^{\circ}\text{C}$ and the average boiling point of sesquiterpenes is $\sim 272\text{ }^{\circ}\text{C}$). At both cases, a sharp change in the mass occurred at $120\text{ }^{\circ}\text{C}$. This can be explained due to the evaporation of the “strongly” adsorbed water molecules. In this temperature, the raw resin sample presents a loss of 3 % of the mass whereas in the dried resin sample, just the 0.14 % of the mass decreased. At the temperatures above than $300\text{ }^{\circ}\text{C}$, and up to $450\text{ }^{\circ}\text{C}$, the plurality of the resin compounds is evaporated (boiling points: neo-abietic acid $433.35\text{ }^{\circ}\text{C}$, abietic acid $439.5\text{ }^{\circ}\text{C}$) and the degradation of the complex polymer structure starts. The third weight loss, from 88 to 99.98 %, above $360\text{ }^{\circ}\text{C}$, in case of raw resin sample, and above

$390\text{ }^{\circ}\text{C}$, in case of dried resin sample, is attributed to the degradation of the structure when finally the 99.8 % of the total weight is lost. As we can see, after the temperature of $480\text{ }^{\circ}\text{C}$, all the differences between the two curves disappear and both curves present exactly the same transition. In this region, $480\text{--}600\text{ }^{\circ}\text{C}$, the mass of the samples almost disappeared and only the 0.02 % of the total mass remained. If the pyrolysis had taken place under oxidation conditions, air, all the mass would have disappeared.

As we can see in Fig. 7, the thermal stability of the dried resin sample is better than the raw sample at overall the temperature zone. This means that the evaporation of the water and of the other volatile compounds, during the increasing of the temperature up to $100\text{ }^{\circ}\text{C}$, is not the only

Fig. 8 FTIR spectra of raw natural resin and dried resin samples



phenomenon that occurs but also some other reformation of the chemical compounds takes place resulting to thermally stronger structure.

3.5 Fourier transform infrared (FTIR) spectrum analysis

The FTIR spectra of both resin samples are shown in Fig. 8. The transmittance wave numbers labeled in blue refer to the dried resin sample, whereas the blank ones refer to the raw resin sample.

As it can be seen (Fig. 8), the IR spectra of the two studied samples are almost identical at overall wavelength region, from 420 up to $3,980\text{ cm}^{-1}$. The presence at the resin (colophony) of carboxyl acids explains the strong stretching vibration of carbonyl which was observed at $1,960\text{ cm}^{-1}$. The characteristic wide band between 2,500 and $3,000\text{ cm}^{-1}$ attributed to the absorption of the stretching OH, characteristic of the carboxyl acid dimer. This region is observable in the case of the raw resin sample, where some moisture amount, humidity, is still adsorbed. The peaks at the $2,545$ and $2,652\text{ cm}^{-1}$ correspond to the overtone stretching of the carboxyl group. The peaks at $1,458$ and $1,385\text{ cm}^{-1}$ appear due to CH_2 and CH_3 bending. In addition, the hydrocarbon structures that contain the three ring structures in the diterpenes give the strong stretching vibration modes C–H of the methyl and methylene group shown at $2,870$ and $2,930\text{ cm}^{-1}$ as well as the C=C bonds appeared at the extra weak peak at $3,080\text{ cm}^{-1}$. Characteristic signals from aromatic groups appear at 795 and 898 cm^{-1} likewise the signal at $1,280\text{ cm}^{-1}$ refers to the O–H bending. Furthermore in the region of $3,100\text{--}3,640\text{ cm}^{-1}$, the antisymmetrical and

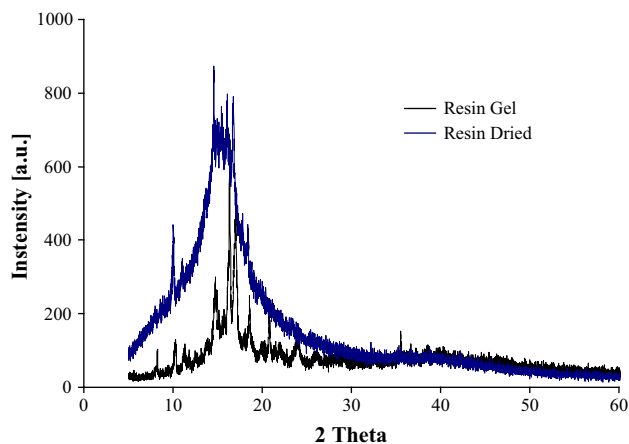


Fig. 9 XRD spectra of the two studied samples

symmetrical stretching modes of water, $\nu_{\text{as}}(\text{O-H})$ and $\nu_{\text{s}}(\text{O-H})$, which appear at $3,477$ and $3,421\text{ cm}^{-1}$, respectively, give an expanded “bell” peak stronger in the case of the raw resin sample which contains moisture from the environmental humidity. These characteristic peaks of the pine resins were also reported previously by other researchers [50–52]. Concluding, as we can see in Fig. 8 the two spectra are almost the same without any intense difference.

3.6 X-ray diffraction

As we can see all the peaks were observed at small angles for both studied samples (Fig. 9). In the case of the raw sample, approximately 21 characteristic peaks were recorded with the main peaks being remarked at 14.78 ,

16.35, 17.06, 18.65, 20.76, 24.13 and 35.52 2θ . On the other hand, the dried resin sample observes a wide “peak” from 5 to 30 2θ where some strong peaks occurred at 10.7, 14.59, 15.4, 16.09, 16.8, 17.82 and 18.36 2θ . Here the evaporation of the high volatile compounds as well as the collapse of the structure and the destruction of the crystallinity, during the drying process, are the main reasons for the disappearance of many peaks and the formation of this main wide peak.

4 Conclusions

The present study was an attempt to establish the possibility to use natural resins as a candidate material for water adsorption applications. For this purpose, water adsorption/desorption isotherm at 22 °C was performed in two resin samples, one raw and one dried, and the kinetics were recorded and analyzed. In order to fit the experimental data with empirical models, both the adsorption isotherm branch and the kinetic curves were fitted with the GAB and the Chapman exponential models, respectively. On the other hand, the thermal properties of the dried sample were increased referred to the raw material, and the local chains conformation seems to be more organized. In addition, the drying process of the natural resin does not change the chemical profile of the material as the FTIR spectra provide. In conclusion, as the water adsorption isotherm shows, the natural resin from *pinus halepensis* pine trees can be a promising renewable material for water adsorption/removal applications, due to the receivable total adsorbate amount of the water.

Acknowledgments E.P. Favvas and A.Ch. Mitropoulos would like to thank the framework NSRF for the funding of the present work. The “NANOCAPILLARY” project (“Thalis” Framework) of the Eastern Macedonia and Thrace Institute of Technology is co-financed by Greece and the European Union in the frame of operational program “Education and lifelong learning investing in knowledge society,” Ministry of Education and Religious Affairs, Culture and Sports. NSRF 2007–2013. The authors would also like to thank Prof. A. Scaltsoyiannes for kindly providing the raw sample.

References

1. P.R. Lewis, C. Gagg, *Forensic Polymer Engineering: why Polymer Products Fail in Service* (Woodhead/CRC Press, Boca Raton, Florida, USA, 2010)
2. S. Mecking, Nature or petrochemistry? Biologically degradable materials. *Angew. Chem. Int. Ed.* **43**, 1078–1085 (2004)
3. V. Sharma, P.P. Kundu, Addition polymers from natural oils—a review. *Prog. Polym. Sci.* **31**, 983–1008 (2006)
4. I. Jantam, A.S. Ahmad, Oleoresins of three *Pinus* species from Malaysian pine plantations. *ASEAN review of biodiversity and environmental conservation* (1999)
5. K.C. Silva Rodrigues-Corrêa, J.C. Lima, A.G. Fett-Neto, Pine oleoresin: tapping green chemicals, biofuels, food protection, and carbon sequestration from multipurpose trees. *Food Energy Secur.* **1**, 81–93 (2012)
6. M.J. Lombardero, M.P. Ayres, P.L. Lorio, J.J. Ruel, Environmental effects on constitutive and inducible resin defenses of *Pinus taeda*. *Ecol. Lett.* **3**, 329–339 (2000)
7. Z. Wang, M.M. Calderon, M.G. Carandang, Effects of resin tapping on optimal rotation age of pine plantation. *J. For. Econ.* **11**, 245–260 (2006)
8. J.J.W. Coppen, J.M. Robinson, L.J. Mullin, Composition of xylem resin from five Mexican and Central American *Pinus* species growing in Zimbabwe. *Phytochemistry* **27**, 1731–1734 (1998)
9. J.J.W. Coppen, C. Gay, D.J. James, J.M. Robinson, N. Supriana, Variability in xylem resin composition amongst natural populations of Indonesian *Pinus merkusii*. *Phytochemistry* **33**, 129–136 (1993)
10. S. Turtola, A.M. Manninen, R. Rikala, P. Kainulainen, Drought stress alters the concentration of wood terpenoids in scots pine and Norway spruce seedlings. *J. Chem. Ecol.* **29**, 1981–1995 (2003)
11. M. Cannac, T. Barboni, L. Ferrat, A. Bighelli, V. Castola, J. Costa, D. Treculd, F. Morandinia, V. Pasqualinia, Oleoresin flow and chemical composition of Corsican pine (*Pinus nigra* subsp. *laricio*) in response to prescribed burnings. *For. Ecol. Manag.* **257**, 1247–1254 (2009)
12. D.T. Tingey, M. Manning, L.C. Grothaus, W.F. Burns, Influence of light and temperature on monoterpene emission rates from slash pine. *Plant Physiol.* **65**, 797–801 (1980)
13. J. Peñuelas, J. Llusà, Short-term responses of terpene emission rates to experimental changes of PFD in *Pinus halepensis* and *Quercus ilex* in summer field conditions. *Environ. Exp. Bot.* **42**, 61–68 (1999)
14. A.G. Ferreira, C.S. Fior, S.C.J. Gualtieri, Oleoresin yield of *Pinus elliptica* Engelm seedlings. *Braz. J. Plant Physiol.* **23**, 313–316 (2011)
15. N.Y. Yang, L. Liu, W.W. Tao, J.A. Duan, L.J. Tian, Diterpenoids from *Pinus massoniana* resin and their cytotoxicity against A431 and A549 cells. *Phytochemistry* **71**, 1528–1533 (2010)
16. X.M. Hu, W.K. Zhang, L.R. Song, L. Hu, G.Z. Zhang, Z.W. Xie et al., *Chinese Materia Medica*, vol. 2 (Shanghai Science and Technology Press, Shanghai, 1998), pp. 303–305
17. R. Tanaka, H. Tokuda, Y. Ezaki, Cancer chemopreventive activity of “rosin” constituents of *Pinus* sp. and their derivatives in two-stage mouse skin carcinogenesis test. *Phytomedicine* **15**, 985–992 (2008)
18. G. Topçu, R. Erenler, O. Çakmak, C.B. Johansson, C. Çelik, H.B. Chai, J.M. Pezzuto, Diterpenes from the berries of *Juniperus excelsa*. *Phytochemistry* **50**, 1195–1199 (1999)
19. P. Mellanen, T. Petänen, J. Lehtimäki, S. Mäkelä, G. Bylund, B. Holmbom, E. Mannila, A. Oikari, R. Santti, Wood-derived estrogens: studies in vitro with breast cancer cell lines and in vivo in trout. *Toxicol. Appl. Pharmacol.* **136**, 381–388 (1996)
20. G. Saxena, C.R. Tudan, A. Merzouk, Tricyclic terpenes of the family of abietic acid as RANTES receptor ligands. US patent, 2003125380 (2003)
21. J. Rubio, J.S. Calderon, A. Flores, Trypanocidal activity of oleoresin and terpenoids isolated from *Pinus oocarpa*. *J. Biosci.* **60**, 711–716 (2005)
22. E. Smith, E. Williamson, M. Zloh, Isopimaric acid from *Pinus nigra* shows activity against multidrug-resistant and EMRSA strains of *Staphylococcus aureus*. *Phytother. Res.* **19**, 538–542 (2005)
23. J. Bohlmann, C.I. Keeling, Terpenoid biomaterials. *Plant J.* **54**, 656–669 (2008)

24. Y. Zhao, J. Yang, B. Qin, Y. Li, Y. Sun, S. Su, M. Xian, Biosynthesis of isoprene in *Escherichia coli* via methylerythritol phosphate (MEP) pathway. *Appl. Microbiol. Biotechnol.* **90**, 1915–1922 (2011)
25. C.G. Tsanaktsidis, E.P. Favvas, A.A. Scaltsoyiannes, S.G. Christidis, E.X. Katsidi, A.V. Scaltsoyiannes, Natural resins and their application in antifouling fuel technology Part I: improving the physicochemical properties of diesel fuel using natural resin polymer as a removable additive. *Fuel. Proc. Technol.* **114**, 135–143 (2013)
26. K.P. Panetsos, *Pinus halepensis* (Mill.) Enzyklopädie der Holzgewächse. 18 (III-1), (1999), p.10
27. R. Croteau, M.A. Johnson, Biosynthesis of terpenoid wood extractives, in *Biosynthesis and Biodegradation of Wood Components*, ed. by T. Higuchi (Academic Press, Orlando, FL, 1985), pp. 379–439
28. G.Th. Tsoumis, *Harvesting forest products*. (Thessaloniki, 1978), pp 135–152
29. D. Moulalis, Variation of resin yield of *Pinus halepensis* in Kassandra Chalkidiki. *Scientific Annals of the School Agriculture and Forestry*, (in Greek, English abstract, 1981), vol. 24–Annex
30. N. Verlet, Commercial aspects, in *Volatile oil crops: their biology biochemistry and production*, eds. R.K.M. Hay, P.G. Waterman (Longman Scientific and Technical, Essex, UK, 1993), pp. 137–174
31. C. Karanikas, V. Walker, A. Scaltsoyiannes, G. Compte, C. Bertrand, High vs. low yielding oleoresin *Pinus halepensis* Mill. trees GC terpenoids profiling as diagnostic tool. *Anna. For. Sci.* **67**, 412–419 (2010)
32. C.G. Tsanaktsidis, S.G. Christidis, E.P. Favvas, A novel method for improving the physicochemical properties of diesel and jet fuel using polyaspartate polymer additives. *Fuel* **104**, 155–162 (2013)
33. E.P. Favvas, K.L. Stefanopoulos, S.K. Papageorgiou, ACh. Mitropoulos, In situ small angle X-ray scattering and benzene adsorption in carbon hollow fiber membranes. *Adsorption* **19**, 225–233 (2013)
34. G. Trovati, E.A.P. Sanches, S.C. Neto, Y.P. Mascarenhas, G.O. Chierice, Characterization of polyurethane resins by FTIR, TGA, and XRD. *J. Appl. Polym. Sci.* **115**, 263–268 (2010)
35. A.D. Roman-Gutierrez, S. Guilbert, B. Cuq, Distribution of water between wheat flour components: a dynamic water vapour adsorption study. *J. Cereal. Sci.* **36**, 347–355 (2002)
36. D.L. Chapman, A contribution to the theory of electrocapillarity. *Philos. Mag.* **25**, 475–481 (1913)
37. S. Brunauer, L.S. Deming, W.E. Deming, E. Teller, On a theory of the van der Waals adsorption of gases. *J. Am. Chem. Soc.* **62**, 1723–1732 (1940)
38. A.J. Fletcher, Y. Yözak, K.M. Thomas, Adsorption and desorption kinetics for hydrophilic and hydrophobic vapors on activated carbon. *Carbon* **44**, 989–1004 (2006)
39. S. Komarneni, R. Pidugu, V.C. Menon, Water adsorption and desorption isotherms of silica and alumina mesoporous molecular sieves. *J. Porous Mater.* **3**, 99–106 (1996)
40. R.W. Mooney, A.G. Keenan, L.A. Wood, Adsorption of water vapor by montmorillonite. I. Heat of desorption and application of BET theory. *J. Am. Chem. Soc.* **74**, 1367–1371 (1952)
41. I. Bravo-Osuna, C. Ferrero, M.R. Jiménez-Castellanos, Water sorption-desorption behaviour of methyl methyl methacrylate-starch copolymers: effect of hydrophobic graft and drying method. *Eur. J. Pharm. Biopharm.* **59**, 537–548 (2005)
42. F. Caturla, M. Molina-Sabio, F. Rodriguez-Reinoso, Adsorption-desorption of water vapor by natural and heat-treated sepiolite in ambient air. *Appl. Clay Sci.* **15**, 367–380 (1999)
43. H. Chen, M. Miao, X. Ding, Influence of moisture absorption on the interfacial strength of bamboo/vinyl ester composites. *Compos. A Appl. Sci. Manuf.* **40**, 2013–2019 (2009)
44. J.N. Coupland, N.B. Shaw, F.J. Monahan, E.D. O’Riordan, M. O’Sullivan, Modeling the effect of glycerol on the moisture sorption behavior of whey protein edible films. *J. Food Eng.* **43**, 25–30 (2000)
45. E. Ayranci, Moisture sorption of cellulose based edible films. *Food/Nahrung* **40**, 274–276 (1996)
46. M.S. Chinnan, H.J. Park, Effect of plasticizer level and temperature on water vapor transmission of cellulose-based edible films. *J. Food Proc. Eng.* **18**, 417–429 (1995)
47. A.B. Dias, C.M.O. Müller, F.D.S. Larotonda, J.B. Laurindo, Biodegradable films based on rice starch and rice flour. *J. Cereal. Sci.* **51**, 213–219 (2010)
48. S. Mali, L.S. Sakanaka, F. Yamashita, M.V.E. Grossmann, Water sorption and mechanical properties of cassava starch films and their relation to plasticizing effect. *Carbohydr. Polym.* **60**, 283–289 (2005)
49. J. Su, A.C. Lua, Effects of carbonisation atmosphere on the structural characteristics and transport properties of carbon membranes prepared from Kapton® polyimide. *J. Membr. Sci.* **305**, 263–270 (2007)
50. R. Imhof, X. Xie, G. Calzaferri, In situ attenuated total reflection FTIR investigations of thin water films in the silanization of ZnSe and Si. *Spectrochim. Acta A* **53**, 981–989 (1997)
51. D. Scalarone, M. Lazzari, O. Chiantore, Ageing behaviour and pyrolytic characterisation of diterpenic resins used as art materials: colophony and Venice turpentine. *J. Anal. Appl. Pyrolysis* **64**, 345–361 (2002)
52. J. Font, N. Salvadó, S. Butí, J. Enrich, Fourier transform infrared spectroscopy as a suitable technique in the study of the materials used in waterproofing of archaeological amphorae. *Anal. Chim. Acta* **598**, 119–127 (2007)